HYDROLOGICAL PROCESSES
Hydrol. Process. **20**, 1027–1046 (2006)
Published online in Wiley InterScience (www.interscience.wiley.com). DOI: 10.1002/hyp.5922

One- and two-dimensional modelling of overland flow in semiarid shrubland, Jornada basin, New Mexico

David A. Howes,[1]* Athol D. Abrahams[2] and E. Bruce Pitman[3]

[1] *Compliance Services International, 7501 Bridgeport Way West, Lakewood, WA 98499, USA*
[2] *Department of Geography, University at Buffalo, The State University of New York, Buffalo, NY 14261, USA*
[3] *Department of Mathematics, University at Buffalo, The State University of New York, 244 Mathematics Building, Buffalo, NY 14260, USA*

Abstract:

Two distributed parameter models, a one-dimensional (1D) model and a two-dimensional (2D) model, are developed to simulate overland flow in two small semiarid shrubland watersheds in the Jornada basin, southern New Mexico. The models are event-based and represent each watershed by an array of 1-m^2 cells, in which the cell size is approximately equal to the average area of the shrubs.

Each model uses only six parameters, for which values are obtained from field surveys and rainfall simulation experiments. In the 1D model, flow volumes through a fixed network are computed by a simple finite-difference solution to the 1D kinematic wave equation. In the 2D model, flow directions and volumes are computed by a second-order predictor–corrector finite-difference solution to the 2D kinematic wave equation, in which flow routing is implicit and may vary in response to flow conditions.

The models are compared in terms of the runoff hydrograph and the spatial distribution of runoff. The simulation results suggest that both the 1D and the 2D models have much to offer as tools for the large-scale study of overland flow. Because it is based on a fixed flow network, the 1D model is better suited to the study of runoff due to individual rainfall events, whereas the 2D model may, with further development, be used to study both runoff and erosion during multiple rainfall events in which the dynamic nature of the terrain becomes an important consideration. Copyright © 2006 John Wiley & Sons, Ltd.

KEY WORDS runoff; overland flow; infiltration; drainage basin; hydrology

INTRODUCTION

Distributed parameter modelling is the most widely used method of modelling runoff in semiarid environments (e.g. Zhang and Cundy, 1989; Goodrich *et al*., 1991; Moore and Grayson, 1991; Vertessy *et al*., 1993; Flanagan and Nearing, 1995; Smith *et al*., 1995). This approach provides a detailed representation of the watershed and an accurate description of the runoff processes using physically based relationships. A watershed is represented as a set of spatial (distributed) elements and the model simulates (1) the hydrologic processes operating within each element (i.e. the conversion of rainfall to runoff), and (2) the flow of water between the elements (i.e. surface runoff).

Distributed parameter models are classified according to (1) the description of the runoff processes and (2) the dimensionality of the flow description. In the first case, models are classified as *deterministic, stochastic*, or *mixed*, depending on the degree of certainty with which the runoff processes are described in the model (Singh, 1996). In the second case, models are classified as either one-dimensional (1D) or two-dimensional (2D). For the simulation of runoff in very small watersheds, both types of model typically employ the kinematic wave approximation to the Saint Venant flow equations. This method involves numerically solving the continuity or mass balance equation using a uniform flow approximation to compute flow velocity.

* Correspondence to: David A. Howes, Compliance Services International, 7501 Bridgeport Way West, Lakewood, WA 98499, USA.
E-mail: dhowes@complianceservices.com

Received 23 April 2003
Accepted 19 January 2005

1D models

1D runoff models are based on the assumption that runoff from a watershed can be treated as a set of 1D flows and that these flows may be integrated to provide a simulated hydrograph at the outlet of the watershed. This concept is generally implemented in a distributed parameter model in one of two ways. The first involves defining the model elements such that they form cascades, whereas the second involves the use of a flow routing algorithm to determine a single outflow direction for each element based on the local topography. The first approach is illustrated by THALES (Grayson *et al*., 1992a) and TOPOG (Vertessy *et al*., 1993), which use the 'stream-tubes' concept of Onstad and Brakensiek (1968), and by KINEROS (Smith *et al*., 1995) and WEPP (Flanagan and Nearing, 1995), which represent hillslopes and channels by cascading planes.

The second 1D approach is illustrated by the model of Scoging *et al*. (1992). In this model, a hillslope or watershed is represented as a grid of square cells, and a flow network is defined using a simple routing algorithm, which allows flow to occur from each cell to one of its eight neighbours. The volume of flow through the network is computed by solving the 1D kinematic wave equation at the centre of each cell. Scoging *et al*. (1992) applied this model to a large runoff plot (35 m long and 18 m wide) on a shrubland hillslope at Walnut Gulch, and Parsons *et al*. (1997) applied a modified version of the model to another large runoff plot (29 m long and 18 m wide) on a grassland hillslope at Walnut Gulch. By comparing simulated hydrographs with observed hydrographs, the two studies showed that the model worked well for cell sizes ranging from 0·5 to 10 m^2.

2D models

In contrast to the 1D models described above, 2D models route flow implicitly and are mathematically more complex. However, according to Zhang and Cundy (1989), 2D models simulate the spatial distribution of overland flow more realistically and with greater accuracy than 1D models do. Goodrich *et al*. (1991) applied a 2D runoff model based on a set of triangular elements to a portion of the Lucky Hills watershed at Walnut Gulch and compared the model results with hydrographs generated by KINEROS. The two models produced similar results. Gao *et al*. (1993) applied a 2D runoff model based on a regular grid spatial structure to the same watershed. Their model was applied without calibration and the results were found to match measured runoff data reasonably well.

Modelling overland flow in the Jornada shrubland

The focus of the present study is on the modelling of runoff processes on the creosotebush (*Larrea tridentata*) shrubland in the Jornada basin, southern New Mexico. This study is part of the Jornada basin Long-Term Ecological Research (LTER) project, which is concerned with the causes and consequences of the widespread replacement of grassland by shrubland in the American Southwest.

Studies concerned with the supply of water to shrubs tend to focus on the role of interception and stemflow (e.g. Navar and Bryan, 1990; Martinez-Meza and Whitford, 1996; Abrahams *et al*., 2005). Furthermore, plant growth models developed by Reynolds *et al*. (1997) to simulate the evolution of shrubland ecosystems are based on the assumption that all of the water reaching a shrub originates as rain falling directly onto the shrub. However, the lateral redistribution of water by overland flow is widely recognized as being critical to plant production of desert ecosystems (Schlesinger and Jones, 1984; Noy-Meir, 1985). On shrubland hillslopes, most shrubs reside on microtopographic mounds a few centimetres high. These cause overland flow in the bare intershrub areas to concentrate in flowpaths, where it diverges and converges around the shrubs in a complex reticular pattern. Nonetheless, significant quantities of water flow onto and off shrub mounds, both adding to and subtracting from the supply of water and nutrients to individual shrubs. These processes have received little attention, in large part due to the lack of a suitable model to simulate overland flow at this scale.

Howes and Abrahams (2003) developed a 2D model to simulate runon at the scale of the individual shrub in two small watersheds in the creosotebush shrubland of the Jornada basin. This 2D model is mathematically

quite complex. Consequently, in this study a 1D model is developed that is mathematically simpler than the 2D model. This model is applied to simulate the runoff in the same two watersheds and the performance of the models is then compared in terms of both the runoff hydrograph and the spatial pattern of overland flow.

In order to simulate overland flow accurately in the Jornada shrubland, the 1D and 2D models were designed to satisfy the following requirements:

1. The model elements must be small enough to discriminate between shrub and intershrub areas.
2. The model must be able to represent accurately the divergence and convergence of flow around individual shrubs.
3. The model should contain the optimum number of parameters to describe the runoff processes accurately, but not in excessive detail.
4. Where possible, the model parameter values should be obtainable from field experiments conducted at the same scale as the model elements.

MODEL DEVELOPMENT

Kinematic wave approximation

The 1D and 2D models are based on the kinematic wave approximation to the Saint Venant flow equations (de Saint Venant, 1871; Ponce, 1991)

$$\frac{\partial h}{\partial t} + \frac{\partial q}{\partial x} = r - f \qquad \text{1D} \tag{1}$$

$$\frac{\partial h}{\partial t} + \frac{\partial q}{\partial x} + \frac{\partial q}{\partial y} = r - f \qquad \text{2D} \tag{2}$$

where h (cm) is the flow depth, t (h) is the time, x and y (cm) are the space increments, r (cm h^{-1}) is the rainfall rate, f (cm h^{-1}) is the infiltration capacity, and q (cm^2 h^{-1}) is the unit discharge, which is computed as

$$q = vh \tag{3}$$

where v (cm s^{-1}) is the flow velocity. Inasmuch as the kinematic wave approximation is based on the assumption that changes in momentum in overland flow are negligible compared with both the gravitational force (which promotes flow) and the frictional forces (which transmit the frictional effects of the surface into the flow) (Baird, 1997), v may be calculated using a uniform flow approximation. Thus, gradually varied, non-uniform, free-surface flow may be visualized as a succession of steady uniform flows (Chow, 1959; Ponce, 1991).

Uniform flow velocity

The 1D and 2D models employ the Darcy–Weisbach flow equation

$$v = \sqrt{\frac{8ghs}{ff}} \tag{4}$$

where g (cm s^{-2}) is the acceleration due to gravity, s is the slope, and ff is the friction factor.

In the kinematic wave approximation, the relationship between q and h is known as the kinematic approximation to the momentum equation (Sherman and Singh, 1976) or the rating equation. This equation has the form

$$q = \alpha h^m \tag{5}$$

where α ($cm^{2-m}\ h^{-1}$) is the kinematic wave friction relationship parameter and m is the slope-friction coefficient. When v is computed using the Darcy–Weisbach equation and s and ff are constant, then α and m are both constants and their values can be obtained from Equation (4) as follows:

$$v = \sqrt{\frac{8ghs}{ff}} = \alpha h^{0{\cdot}5} \tag{6}$$

where $\alpha = \sqrt{8gs/ff}$. Therefore, from Equation (3)

$$q = vh = \alpha h^{1{\cdot}5} \tag{7}$$

Thus, m in Equation (5) is equal to 1·5.

Infiltration

Infiltration is described in the model using the storage-based Smith–Parlange equation (Smith and Parlange, 1978; Woolhiser *et al*., 1990)

$$f = \frac{K_s\ e^{F/B}}{e^{F/B} - 1} \quad f > 0 \tag{8}$$

where f (cm h^{-1}) is the infiltration capacity, K_s (cm h^{-1}) is the saturated hydraulic conductivity, F (cm) is the infiltrated depth, and B (cm) is a soil storage parameter (Freeze, 1980) defined by

$$B = \frac{S^2}{2K_s} \tag{9}$$

where S (cm $h^{-0{\cdot}5}$) is the sorptivity accounting for both capillary suction and initial conditions.

If the soil properties are the same throughout the watershed and all points receive the same amount of rainfall, then ponding occurs at all points simultaneously. However, most soil properties are highly variable over short distances (e.g. Nielsen *et al*., 1973; Springer and Cundy, 1987), and this spatial variability may give rise to runon infiltration. Runon infiltration occurs when runoff generated in an upslope area encounters a downslope area where ponding has not occurred. In the latter area, the rainfall excess is still negative, so the soil still has infiltration capacity to satisfy. Some or all of this unsatisfied capacity may be filled by runon. The effect of runon infiltration is to increase the infiltrated depth, and thus accelerate ponding, causing runoff to occur earlier than it otherwise would (Scoging *et al*., 1992).

Using Equation (8) and allowing for runon infiltration, the infiltration rate i (cm s^{-1}) is computed as either

$$i = q_r + r \text{ for } f > q_r + r \tag{10}$$

or

$$i = f \text{ for } f \leq q_r + r$$

where q_r (cm h^{-1}) is the runon per unit surface area.

1D MODEL

Numerical solution scheme

In the 1D runoff model, a first-order 1D finite-difference scheme is used to solve the 1D kinematic wave equation (Equation (1)). The finite-difference form of this equation is

$$\frac{h_i^{t+\Delta t} - h_i^t}{\Delta t} + \frac{q_i^t - q_{i-\Delta x}^t}{\Delta x} = ex_i^t \tag{11}$$

where subscript i is a spatial node on the flowpath, Δx is the space increment, and $ex = r - f$. This scheme is known as a backward-space scheme because the space differencing occurs backwards with respect to the direction of flow (i.e. upslope).

Rearranging Equation (11), and solving for h at the next time step gives

$$h_i^{t+\Delta t} = h_i^t - \frac{\Delta t}{\Delta x}(q_i^t - q_{i-\Delta x}^t) + ex_i^t \tag{12}$$

Stability

The numerical solution to the 1D kinematic wave equation can be prevented from becoming unstable by the use of two stability constraints, both of which must be satisfied. The first of these is the Courant condition, a stability measure relating u, Δt, and Δx, which refers to the left side of Equation (1).

The Courant condition states that the scheme will remain stable as long as

$$\frac{u\Delta t}{\Delta x} \leq 1 \tag{13}$$

The left side of this equation is referred to as the Courant number.

In the 1D numerical solution scheme, Δt can be varied at each time step in response to instability, and also as a means of improving efficiency. Should the Courant number exceed unity, the value of Δt is reduced and the value of h recalculated.

The efficiency of the numerical scheme can also be improved by choosing as large a value of Δt as possible while ensuring that the value used will not cause the scheme to become unstable. A suitable value of Δt can be obtained by rearranging Equation (13) to give

$$\Delta t = C\frac{\Delta x}{u} \tag{14}$$

where C is the Courant coefficient, and $0 < C < 1$.

Using Equation (14), Δt will vary with the flow conditions. If conditions are changing rapidly, Δt will be very small, but if conditions are changing more slowly, Δt will have a larger value. Thus, when time steps are selected according to the Courant condition, the numerical scheme is able to respond to the variability present in the analytical solution.

The value of C is generally fixed, but this is not required. In many applications using the Courant condition, $C = 0{\cdot}9$ is an appropriate choice. However, the value of Δt provided by Equation (14) may be too large in situations where flow conditions change extremely rapidly, causing the solution scheme to become unstable. As long as the Courant condition is checked at the end of each time step, this situation can be addressed by recalculating h using a smaller Δt. If the estimates of Δt are consistently too large, then a smaller value of C can be used in the scheme to reduce the number of times that h must be recalculated. In testing the models for the Jornada shrubland, it was found that C had to be as low as $0{\cdot}1$. This is because the velocity of overland flow in the shrubland can be high (in excess of $1{\cdot}3$ m s^{-1}) and can change rapidly due to a number of factors, including the convergence and divergence of flow around shrub mounds and sudden variations in rainfall intensity during summer thunderstorms.

The second stability constraint applies to the source term (the right-hand side of Equation (1)). In general, if A is the magnitude of the source term, then the numerical scheme will be stable as long as

$$\Delta t < \frac{1}{A} \tag{15}$$

As with the Courant condition, problems may arise if conditions change rapidly. Therefore, requiring that

$$\Delta t < \frac{0{\cdot}1}{A} \tag{16}$$

is more reliable when modelling highly variable flow conditions typical of the Jornada shrubland.

Flow network

For the 1D model, flow networks are computed using the algorithm of Tarboton (1997). This algorithm was selected (1) because of its ability to represent effectively the diverging and converging flowpaths of the Jornada shrubland and (2) because it is a robust procedure which is based on a simple grid structure and is relatively insensitive to grid orientation.

The Tarboton algorithm takes as input a digital elevation model (DEM) and, for every cell in the DEM, calculates a flow vector for each of eight triangular facets radiating from the centre of the cell. The steepest downslope vector from all eight facets is taken as the flow vector for the cell. Flow is then apportioned between a maximum of two downslope cells according to a procedure described in Tarboton (1997).

Since it includes only one space dimension, the 1D kinematic wave equation applies to flow along a 1D flowpath, which implies that any point along the flowpath can have only one inflow and one outflow. However, Scoging *et al*. (1992) and Parsons *et al*. (1997) showed that it is acceptable to treat the inflow to a spatial node as the sum of several inflows and also to divide the outflow from a spatial node between a number of cells. The 1D numerical scheme may, therefore, be used to compute the flow depth at each node in the diverging and converging flow network produced using the Tarboton algorithm.

Initial and boundary conditions

At the beginning of a simulated rainstorm, the value of h is set to zero at all nodes in the flow network, and the antecedent moisture is specified by assigning an initial value to F in the Smith–Parlange equation (Equation (8)).

2D MODEL

Numerical solution scheme

The spatial and temporal variations in flow depth are simulated in the model by numerical solution of the 2D kinematic wave equation (Equation (2)) using a second-order accurate predictor–corrector finite-difference scheme developed by Davis (1988). The Davis algorithm was originally designed for problems in computational fluid dynamics and provides greater spatial and temporal accuracy than the 1D numerical schemes used previously in modelling overland flow (e.g. Scoging *et al*., 1992; Parsons *et al*., 1997). The ability of the algorithm to capture nonlinear shocks and expansion waves smoothly and accurately makes it well suited to modelling the rapidly changing flow conditions typical of the Jornada shrubland. The model developed by Howes and Abrahams (2003) represents the first application of the Davis algorithm to modelling overland flow.

The Davis algorithm can be summarized as follows. For each cell in the model grid, the flow depth is calculated at each time step by taking into account the flows between the cell and each of the eight neighbouring cells. Flows in the cardinal directions are calculated explicitly, whereas those between the cell and its diagonal neighbours are calculated implicitly. A simplified version of the equations underlying the algorithm is provided below. The reader is referred to Davis (1988) for further details. The simplified numerical scheme discussed below (Equation (19)) is not stable in its own right, but it is made stable by minor modifications included in the Davis scheme.

Second-order accuracy in the spatial dimensions is obtained using centre-differencing. With the value of the source term $(r - f)$ set to zero, Equation (2) can be expressed as

$$\frac{h_{i,j}^{t+\Delta t} - h_{i,j}^{t}}{\Delta t} + \frac{q_{i+\Delta x,j}^{t} - q_{i-\Delta x,j}^{t}}{2\Delta x} + \frac{q_{i,j+\Delta y}^{t} - q_{i,j-\Delta y}^{t}}{2\Delta y} = 0 \tag{17}$$

If the flow velocity in the x direction is denoted by a and that in the y direction is denoted by b using Equation (3), then Equation (17) can be rewritten as

$$\frac{h_{i,j}^{t+\Delta t} - h_{i,j}^{t}}{\Delta t} + \frac{a}{2\Delta x}\left(h_{i+\Delta x,j}^{t} - h_{i-\Delta x,j}^{t}\right) + \frac{b}{2\Delta y}\left(h_{i,j+\Delta y}^{t} - h_{i,j-\Delta y}^{t}\right) = 0 \tag{18}$$

which can be solved for $h_{i,j}^{t+\Delta t}$ to give

$$h_{i,j}^{t+\Delta t} = h_{i,j}^{t} - a\frac{\Delta t}{2\Delta x}(h_{i+1,j}^{t} - h_{i-1,j}^{t}) - b\frac{\Delta t}{2\Delta y}(h_{i,j+1}^{t} - h_{i,j-1}^{t}) \tag{19}$$

Second-order accuracy in space is obtained using the midpoint rule in which h for a cell is computed in two steps: at the midpoint of a given time step (the predictor step) and at the end of the time step (the corrector step).

In the predictor step, h is estimated for each of the four cardinal neighbours of a cell, and these midtime values are used to compute h for the cell in the corrector step:

$$h_{i,j}^{t+\Delta t} = h_{i,j}^{t} - a\frac{\Delta t}{2\Delta x}(h_{i+1,j}^{t+\Delta t/2} - h_{i-1,j}^{t+\Delta t/2}) - b\frac{\Delta t}{2\Delta y}(h_{i,j+1}^{t+\Delta t/2} - h_{i,j-1}^{t+\Delta t/2}) \tag{20}$$

Thus, the calculation of $h_{i,j}^{t+\Delta t}$ takes into account not only the components of flow along the axes, but also the components of flow from the diagonal cells $(i-1, j+1)$, $(i+1, j+1)$, $(i+1, j-1)$ and $(i-1, j-1)$ through the calculation of the midtime h values in the predictor step. As for the 1D model, instability of the numerical solution scheme is avoided by checking the Courant condition (Equation (13)) and the source term stability measure (Equation (16)) at the end of each time step and, if necessary, recomputing the h values for the time step using a new time increment.

Initial and boundary conditions

The value of h is set to zero in all cells at the beginning of a simulation run, and the antecedent moisture is specified by assigning an initial value to F in the Smith–Parlange equation (Equation (8)). At the end of each time step during a model run, h is set to zero in all cells along the boundary of the model grid. In other words, the boundary cells act as permanent sinks. In general, this procedure is likely to have a negligible effect on the simulation of runoff in a watershed as long as the boundary cells are several metres from the watershed boundary.

PARAMETERIZATION

Parameterization and calibration of physically based distributed runoff models have been the subject of much discussion. This discussion has centred on the appropriate number of parameters to be used in such models and, in particular, on the number of parameters that require adjustment during calibration (e.g. Beven, 1989; Grayson *et al*., 1992b; Refsgaard, 1997). In general, as the number of parameters in a model increases, so too does the degree of interdependence between the parameters and, as a consequence, the chance of error. Additionally, as the number of parameters requiring adjustment during calibration increases, the greater is the likelihood that the model output will not be a unique and accurate representation of the runoff process (Beven, 1989). These potential problems can be avoided by adherence to the following recommendations (Beven, 1989; Refsgaard and Storm, 1996; Refsgaard, 1997):

1. The number of parameters should be kept to a minimum while retaining the ability to represent the runoff processes accurately.

2. Values for as many of the parameters as possible should be determined from field data.
3. The parameter values obtained from field experiments should be collected at the same scale as the model elements to which they will be assigned.

In accordance with the first of these recommendations, the number of parameters employed in the 1D and 2D runoff models was limited to six. Recommendations 1 and 2 are discussed in the following sections, which describe the study watersheds and the spatial representation of these watersheds.

Study watersheds

The 1D and 2D models are parameterized for two small watersheds located in the creosotebush shrubland at the foot of Mount Summerford on the west side of the Jornada basin. The two watersheds differ slightly in terms of their relief, surface properties, and the nature of the shrubs. These differences, however, are typical of the variation across the creosotebush shrubland at Jornada. The watersheds are referred to as the north and south watersheds.

The north watershed (Figure 1), which has an area of 775 m^2, lies ~750 m downslope from Mount Summerford. The shrubs in this watershed have an average height of 1·34 m and average canopy diameter of 1·59 m. Apart from occasional small forbs, vegetation is generally absent from the intershrub areas. The soil underlying the shrub and intershrub surfaces is a Typic Haplargid loamy sand (Schlesinger *et al*., 1999); the rills have sandy beds that, like the loamy sand, have a gravel content of <5% (by weight).

Figure 1. Map of the north watershed showing 5 cm contours, rills, and shrubs

All of the shrubs in the north watershed are underlain by the same type of soil, but this soil may be bare, covered by grass (*Muhlenbergia porteri*), or covered by litter. The presence of vegetation or litter increases the friction encountered by water flowing under the shrubs. This increased friction causes a reduction in flow velocity, thus increasing the likelihood that the water will infiltrate rather than run off into the surrounding intershrub area. In addition, sub-canopy vegetation may enhance infiltration by increasing soil organic matter and macroporosity through root decomposition and faunal activity (Abrahams *et al*., 2005). Since the differences in ground cover affect the amount of runoff in the watershed, it was necessary to distinguish between the three surface types in the modelling.

The south watershed (Figure 2), which has an area of 889 m^2, is situated ~1·2 km southeast of the north watershed. Like the north watershed, it is located on Typic Haplargid soils (Schlesinger *et al*., 1999) but has a more incised rill network. The creosotebush in this watershed have an average height of 0·89 m and average canopy diameter of 0·92 m. Both the shrub mounds and intershrub areas are bare and consist of loamy sand, and the rill beds consist of sand. In contrast to the north watershed, gravel constitutes 30% of the rill and intershrub soils, and 5% of the shrub soil.

As shown in Table I, the parameter values for the north and south watersheds were acquired from watershed surveys, watershed monitoring, and rainfall simulation experiments. The procedures used to obtain the data for s, r K_s, B, F_i, and ff are described in detail in Howes and Abrahams (2003) and, therefore, will not be discussed here.

Spatial representation of the watersheds

For the purpose of the modelling, each watershed is represented by a grid of 1 m^2 cells. This guarantees that, apart from the creation of the 1D flow network, the parameterization process is virtually identical for the

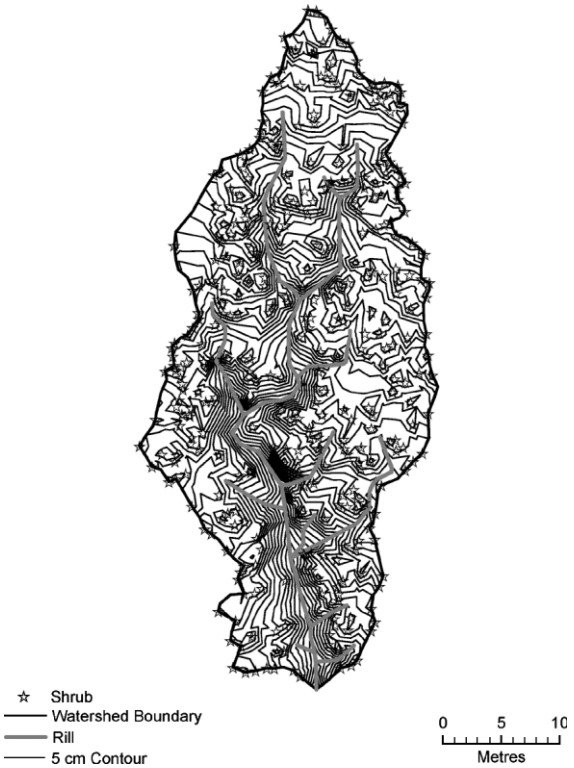

Figure 2. Map of the south watershed showing 5 cm contours, rills, and shrubs

Table I. Model parameters and the source of their values

Parameter	Symbol	Source
Slope	s	DEM based on field survey
Rainfall	r	Tipping-bucket rain gauge attached to data logger
Saturated hydraulic conductivity	K_s	Rainfall simulation experiments
Soil storage parameter	B	Model fit using rainfall simulation data
Initial infiltrated depth	F_i	Based on rainfall data
Darcy–Weisbach friction factor	ff	Friction plot experiments or model fit to rainfall simulation data

two models and that the spatial distributions of runoff properties, such as flow depth and discharge, generated by one model can be directly compared with those generated by the other.

A cell size of 1 m^2 was chosen to correspond to the average area of the shrub mounds in the south watershed. Although the shrub mounds in the north watershed are about twice as large, the same cell size was used in both watersheds to facilitate comparison of the results. The use of small cells is also in accord with the second and third recommendations with regard to the parameterization.

In distributed parameter modelling, it is not uncommon for parameter values obtained for a small area to be assigned to model cells representing much larger areas (e.g. Bathurst, 1986). This is problematic, because the spatial averaging of model parameters, such as K_s and ff, will be greater for a model cell than for the area over which the parameter was measured (Beven, 1989; Grayson *et al*., 1992b). The use of 1 m^2 cells in the present study makes it feasible to conduct field experiments to parameterize the model at the same scale as the model cells. This ensures that the spatial averaging of model parameters is the same in the model cells as it is in reality.

For each watershed, the model grid was aligned with the long axis of the watershed; and the grid was positioned such that the flume at the outlet of the watershed was located in the centre of a cell. Simulations with other alignments showed that the main findings were insensitive to grid alignment.

Because the runoff processes operating beneath shrubs contrast sharply with those operating between shrubs, each cell was classified as either shrub or intershrub. The north watershed shrub cells were then classified as bare, grass-covered, or litter-covered. All south watershed shrub cells were classified as bare. Rill surfaces resembled intershrub surfaces and were, therefore, classified as such.

The ArcInfo Geographic Information System package (ESRI, 1998) was used to create a DEM for each watershed from the survey data. The Tarboton algorithm was then applied to the DEMs to generate the flow networks shown in Figures 3 and 4.

MODEL RESULTS

The predictive abilities of the two models are compared by examining runoff hydrographs and the spatial distribution of overland flow in the two watersheds. In this paper, model output is compared for two storms, but hydrographs for six storms are compared by Howes and Abrahams (2003).

Figure 5 to 8 show the hydrographs predicted by the 1D and 2D models for storms on 30 July and 14 August 1997. Inspection of these hydrographs suggests the following tendencies:

1. The hydrographs for the 30 July storm in the south watershed show that both models are, on some occasions, capable of providing accurate predictions of the hydrographs.
2. The 1D model tends to overpredict observed peak discharges, whereas the 2D model tends to underpredict observed peak discharges.
3. For the north watershed, both models accurately predict the time of peak runoff, whereas for the south watershed, the model predictions tend to lag behind the observed peak discharges.

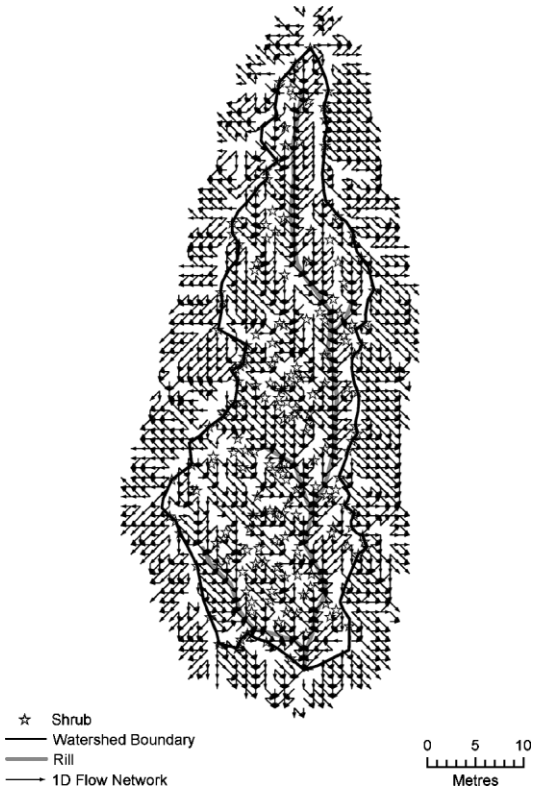

Figure 3. Flow network for the north watershed generated by the Tarboton algorithm

4. There is a tendency for the 1D model to predict higher peak discharges than the 2D model. This tendency is particularly strong and implies that the 1D model concentrates overland flow more quickly and predicts greater flow velocities than the 2D model does. This implication is evaluated by examining the spatial distribution of overland flow in the watersheds.

Spatial distribution of overland flow

Greyscale images representing the spatial distribution of flow depth at the time of peak discharge for the 30 July 1997 storm are shown for the north watershed in Figures 9 and 10 and for the south watershed in Figures 11 and 12. The rills surveyed are also shown in each figure. The images suggest that the models simulate the spatial pattern of flow depth in each watershed well, although the differences between the 1D and 2D representations of the runoff processes are clear. In the 1D model, much of the flow is confined to narrowly defined flowpaths, especially along the main rill in each watershed, whereas the flow exhibits much greater dispersion when represented by the 2D model. Except in a few places in each watershed, the depth of flow in cells along the watershed boundary is small. However, as will be discussed later, some flow across the boundary does occur.

A section of the south watershed is shown in Figures 13 and 14 in order to provide a detailed view of the 1D and 2D flow patterns. The depth of flow in the main channel is about 3·6 cm in the 1D representation, whereas flow is distributed over a wider area in the 2D representation and is, therefore, only about 1·85 cm deep at the same point. This 2D representation of the flow in the rills is less realistic than that for the 1D model, especially in the south watershed. In reality, the rills in this watershed are well defined and flow is generally confined to a width of less than 1 m. Thus, in the case

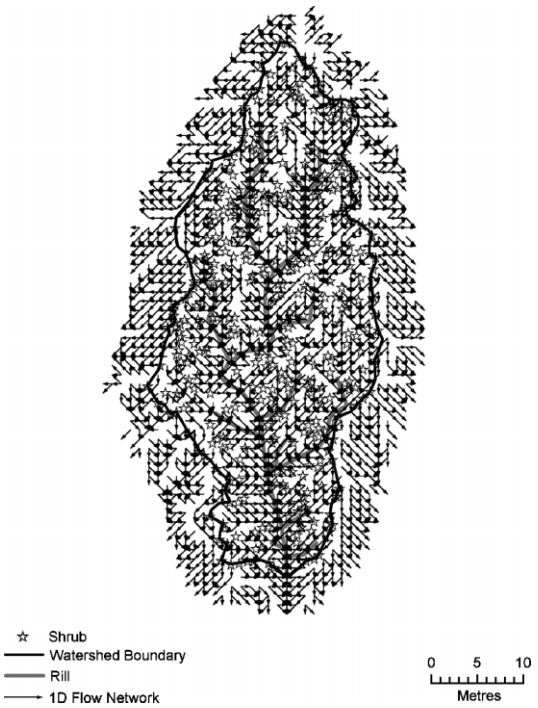

Figure 4. Flow network for the south watershed generated by the Tarboton algorithm

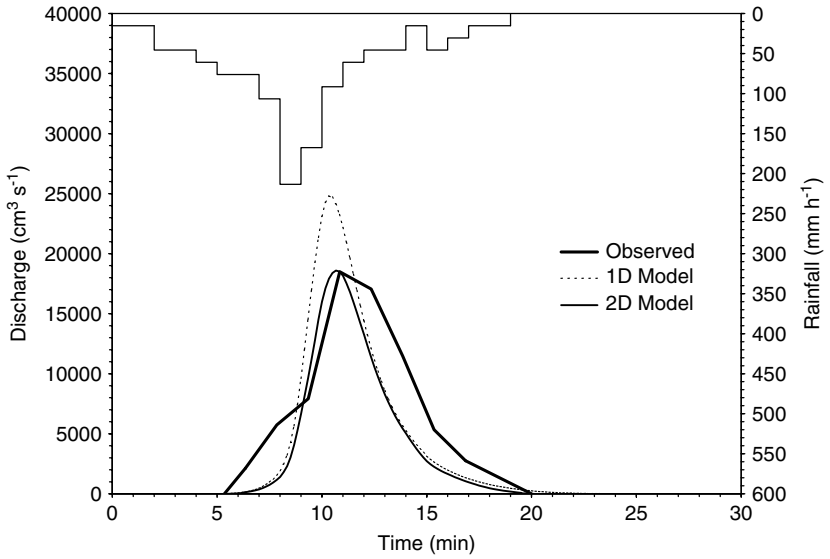

Figure 5. North watershed observed and simulated hydrographs for the 30 July 1997 storm

of rill cells, the discrete and well-defined flowpaths that are specified by the Tarboton algorithm are more realistic than the dispersive flow pattern simulated by the 2D model. The 2D model, however, provides a more realistic representation of the flow on the hillslopes between the rills than does the 1D model.

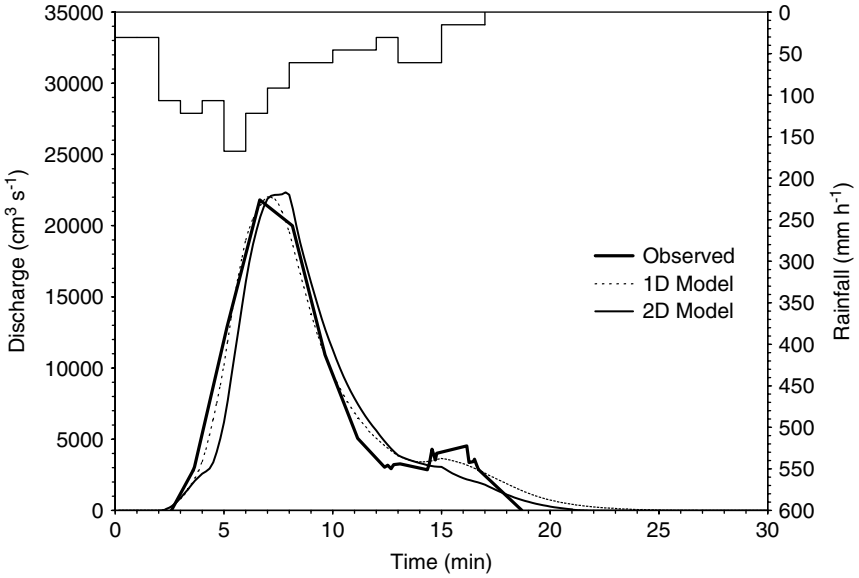

Figure 6. South watershed observed and simulated hydrographs for the 30 July 1997 storm

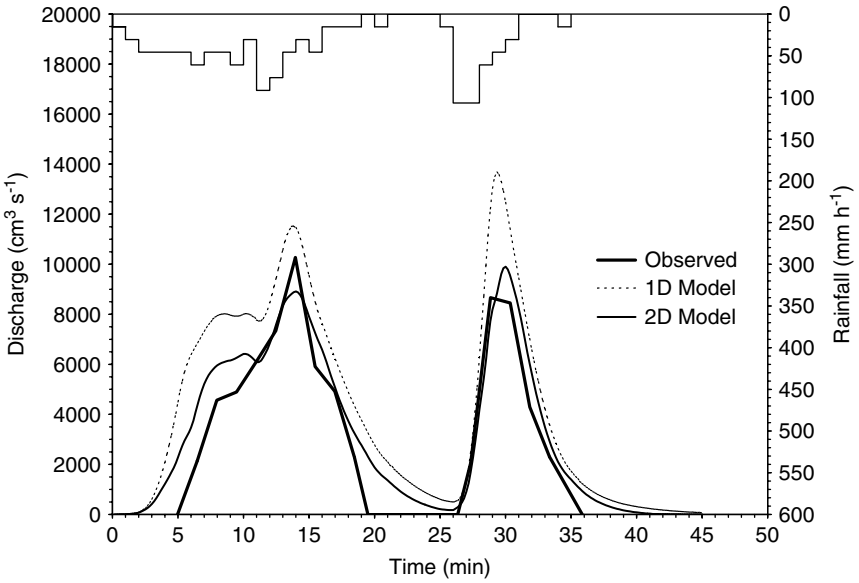

Figure 7. North watershed observed and simulated hydrographs for the 14 August 1997 storm

Differences between the output from the 1D and 2D models

Flow routing, infiltration, and flow resistance. The primary differences between the performances of the 1D and 2D runoff models relate to flow routing, as illustrated by the flow depth images discussed above. In general, the total distance travelled by overland flow in a watershed, which can be referred to as the cumulative flow distance, is smaller when the flow is represented one-dimensionally than when it is represented two-dimensionally.

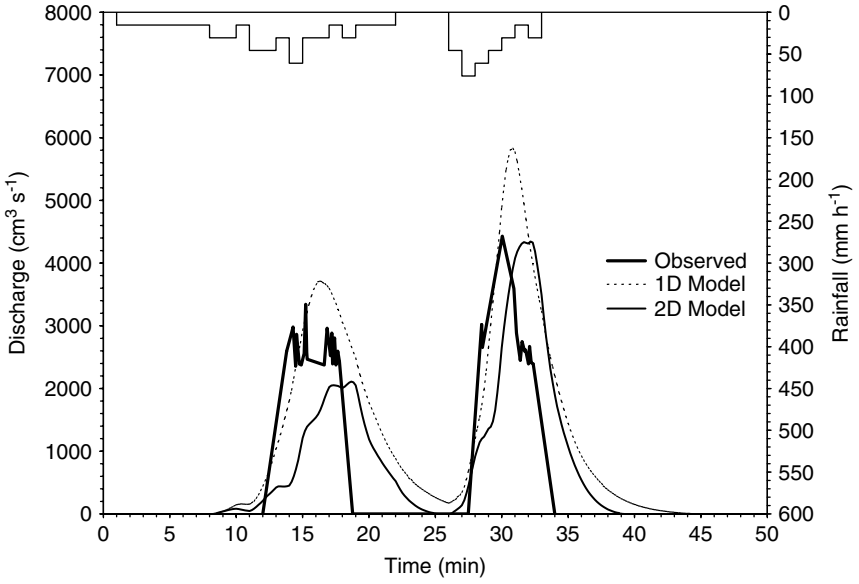

Figure 8. South watershed observed and simulated hydrographs for the 14 August 1997 storm

The two main consequences of differences in the cumulative flow distance relate to infiltration and flow resistance. An increase in the cumulative flow distance is generally accompanied by an increase in the opportunity for water to infiltrate. The predicted hydrographs suggest that the total volume of infiltration estimated by the 1D model is consistently less than that estimated by the 2D model. With a lower cumulative flow distance, the flow encounters lower overall resistance, which causes the runoff hydrograph to be more flashy than it would be if the flowpaths were longer. Except in the case of the 30 July 1997 south watershed storm, the peak runoff predicted by the 1D model typically occurs earlier and has a greater magnitude than that predicted by the 2D model. The distinction between the 1D and 2D hydrographs is less for the 30 July 1997 south watershed storm because of the low values of K_s in this watershed and the significant volume of rainfall associated with the storm. The watershed became saturated very quickly in both model simulations. At saturation, the amount of infiltration is no longer the dominant factor affecting the model output, and differences between the hydrographs are related only to the more minor effect of flow resistance.

Leakage along the watershed boundary. Differences between the 1D and 2D model hydrographs also reflect the way each model represents leakage along the boundary of the watershed. Although an attempt was made to find watersheds with well-defined boundaries, the relief in both the north and south watersheds is so small and the slopes are so gentle that some leakage along the watershed boundary is inevitable. For each simulation run, the relative amount of water leaving the watershed along the boundary was estimated from a balance check. The water balance was computed at the end of each run by subtracting the total volumes of runoff, infiltration, and water left on the watershed surface, from the total volume of rainfall.

In the case of the 30 July 1997 storm (Figures 5 and 6) for the 1D model, 0·75% of the total rainfall in the north watershed left the watershed at points other than the outflow. For the same storm, however, a 5·33% loss across the boundary was simulated by the 2D model. The increased loss simulated by the 2D model and the increased volume of infiltration simulated by this model account for the differences between the 1D and 2D hydrographs for the storm.

By contrast, for the same storm at the south watershed, the 1D model simulates a 3·74% loss of water across the boundary, whereas the 2D model simulates a loss of only 1·62%. The increased runoff simulated by the 1D model is adequately explained by the lower amount of infiltration simulated by this model.

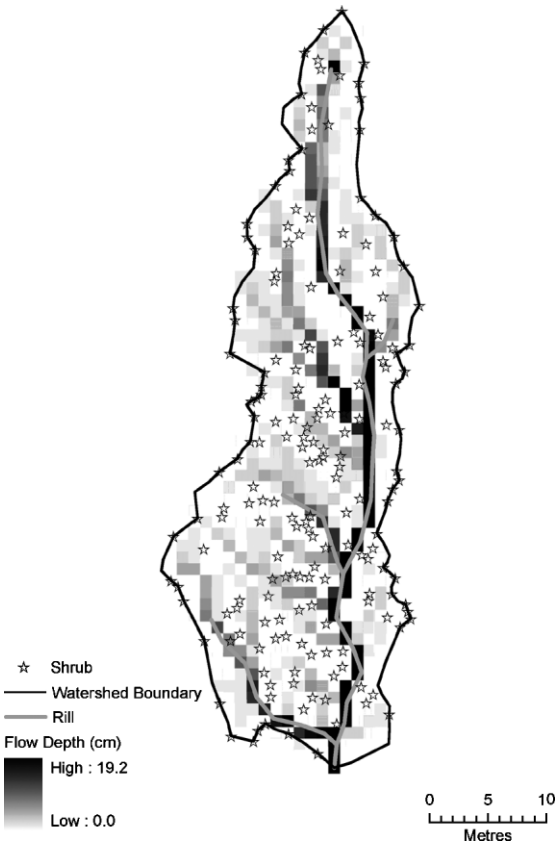

Figure 9. Spatial distribution of flow depth in the north watershed at peak discharge, 30 July 1997, simulated by the 1D model. The rills and watershed boundary are defined by the survey data

1D versus 2D models

When comparing the 1D and 2D models developed in this study it is important to bear in mind the fundamental differences between the models. The second-order accurate numerical scheme employed to solve the kinematic wave equation in the 2D model has a sound mathematical and physical basis. The model is versatile, in that the flow network for a watershed does not have to be specified in advance and the numerical scheme is able to integrate converging flows smoothly, despite the rapidly changing flow conditions typical of the north and south watersheds.

In contrast to the 2D model, the 1D model is based on a flow structure that is fixed for the duration of a runoff event and employs a somewhat crude application of a first-order accurate numerical scheme to solve the kinematic wave equation and thus compute the volume of flow through the network. The application of the numerical scheme is crude because it assumes (1) that inflows to a cell can be summed and treated as if they had originated in one place and (2) that flow from a cell may be simply divided between two downslope cells according to the direction of a single slope value computed for the cell. As a result of these assumptions, flow integration is carried out less smoothly than in the 2D model. With respect to the spatial distribution of overland flow, the 1D model performs better than the 2D model where flow is concentrated into well-defined flowpaths (e.g. rills), whereas the 2D model is better suited to simulating dispersed interrill flow on hillslopes with no rills or channels. This suggests that, in order to model overland flow in the shrubland environment more realistically, it may be appropriate to combine a 2D model for interrill flow with a 1D model for rill

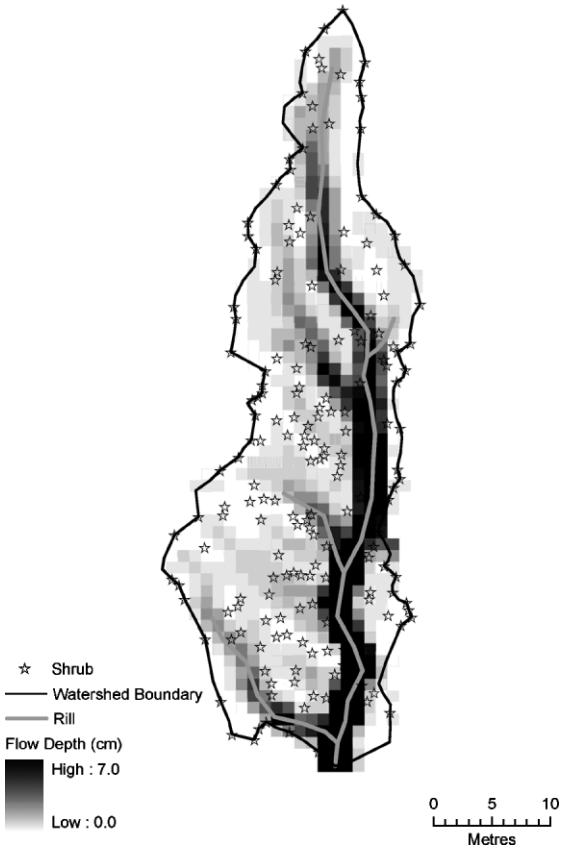

Figure 10. Spatial distribution of flow depth in the north watershed at peak discharge, 30 July 1997, simulated by the 2D model

flow. The idea of using different (coupled) models for overland flow and rill or channel flow is not new, but in existing runoff models, such as KINEROS and WEPP, both the overland flow and channel flow models are usually represented using 1D models.

The simulation results presented in this study suggest that, despite their differences, both the 1D and the 2D models have much to offer as tools for the large-scale study of overland flow. Because it is based on a fixed flow network, the 1D model is better suited to the study of runoff due to individual rainfall events, whereas the 2D model may, with further development, be used to study both runoff and erosion during multiple rainfall events in which the dynamic nature of the terrain becomes an important consideration. Slope values can be recomputed at any time during the operation of the 2D model in response to erosion and deposition.

CONCLUSIONS

Two distributed parameter models, a 1D model and a 2D model, are developed to simulate overland flow in two small semiarid shrubland watersheds in the Jornada basin, southern New Mexico. The models are event based and represent each watershed by an array of 1 m^2 cells, in which the cell size is approximately equal to the average area of the shrubs.

Each model uses only six parameters, for which values are obtained from field surveys and rainfall simulation experiments. In the 1D model, a flow network is generated for a watershed using the Tarboton (1997) algorithm and flow volumes through this network are computed by a simple finite-difference solution

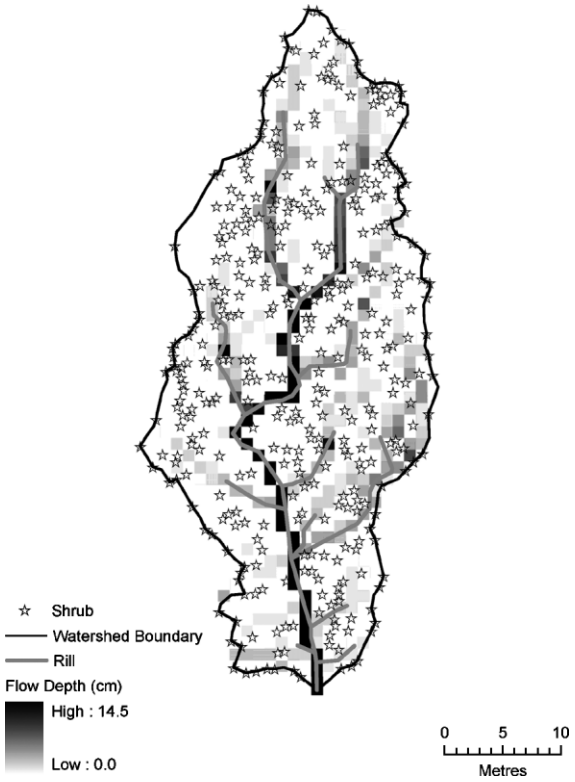

Figure 11. Spatial distribution of flow depth in the south watershed at peak discharge, 30 July 1997, simulated by the 1D model

to the 1D kinematic wave equation. In the 2D model, flow directions and volumes are computed by a second-order predictor–corrector finite-difference solution to the 2D kinematic wave equation, in which flow routing is implicit and may vary in response to flow conditions.

The models are compared in terms of the runoff hydrograph and the spatial distribution of runoff for two storms. The results show that both models are capable of providing accurate predictions of the runoff from the watersheds. However, the 1D model concentrates overland flow more quickly and predicts greater flow velocities than the 2D model does. As a result, the 1D model tends to overpredict observed peak discharges, whereas the 2D model tends to underpredict observed peak discharges. Despite these differences, the simulation results suggest that both the 1D and the 2D models have much to offer as tools for the large-scale study of overland flow. Because it is based on a fixed flow network, the 1D model is better suited to the study of runoff due to individual rainfall events, whereas the 2D model may, with further development, be used to study both runoff and erosion during multiple rainfall events in which the dynamic nature of the terrain becomes an important consideration.

ACKNOWLEDGEMENTS

This research was supported by the National Science Foundation Jornada Basin Long-Term Ecological Research (LTER) project (DEB 94-11971) and the National Center for Geographic Information and Analysis (SBR 88-10917), University at Buffalo, The State University of New York. We are grateful to John Anderson and the LTER technicians at New Mexico State University, Las Cruces, for operating and maintaining the hydrometeorological instruments in the two watersheds; to Kris Havstad and staff at the USDA-ARS Jornada

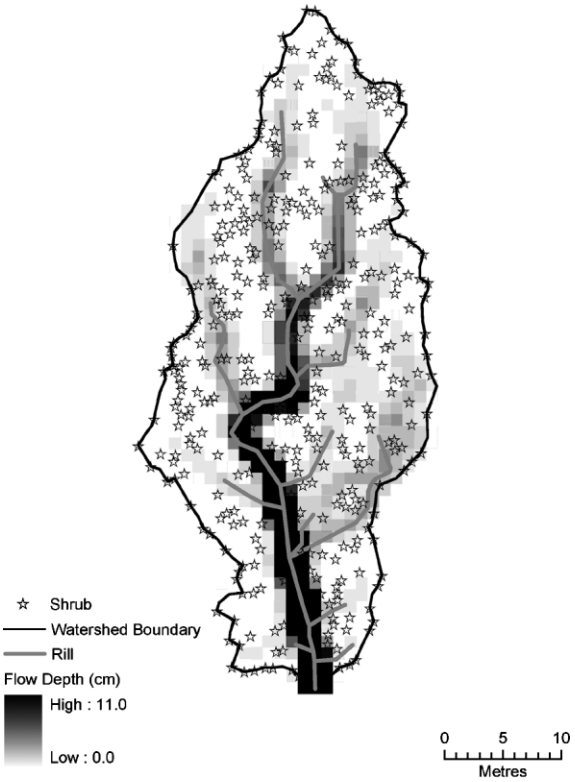

Figure 12. Spatial distribution of flow depth in the south watershed at peak discharge, 30 July 1997, simulated by the 2D model

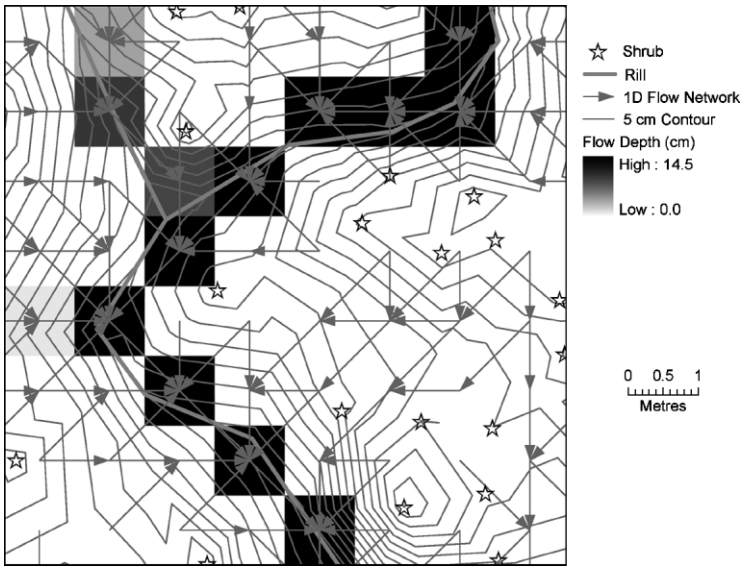

Figure 13. Detailed view of the spatial distribution of flow depth in the south watershed at peak discharge, 30 July 1997, simulated by the 1D model

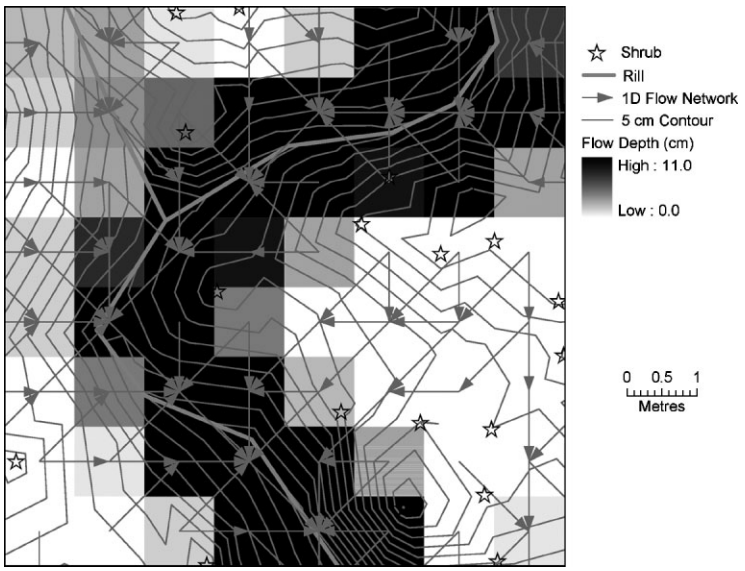

Figure 14. Detailed view of the spatial distribution of flow depth in the south watershed at peak discharge, 30 July 1997, simulated by the 2D model

Experimental Range for building the supercritical flumes and providing the tanker truck; and to Melissa Neave, Scott Rayburg, and Scott McCabe, University at Buffalo, for their assistance with the fieldwork.

REFERENCES

Abrahams AD, Neave M, Schlesinger WH, Wainwright J, Howes DA, Parsons AJ. 2005. Fluxes of water and materials: processes and controls. In *Structure and Function of a Chihuahuan Desert Ecosystem: The Jornada Basin Long-Term Research Site*, Schlesinger WH, Huenneke L, Havstad K (eds). Oxford University Press: Oxford, UK.

Baird AJ. 1997. Overland flow generation and sediment mobilisation by water. In *Arid Zone Geomorphology: Process, Form and Change in Drylands*, second edition, Thomas DSG (ed.). Wiley: New York; 153–215.

Bathurst JT. 1986. Physically-based distributed modelling of an upland catchment using the Système Hydrologique Européen. *Journal of Hydrology* **87**: 79–102.

Beven K. 1989. Changing ideas in hydrology—the case of physically-based models. *Journal of Hydrology* **105**: 157–172.

Chow VT. 1959. *Open Channel Hydraulics*. McGraw-Hill: London.

Davis SF. 1988. Simplified second-order Godunov-type methods. *SIAM Journal of Scientific and Statistical Computing* **9**: 445–473.

ESRI. 1998. *ArcInfo User Manual*. Environmental Systems Research Institute, Inc.: Redlands, CA.

Flanagan DC, Nearing MA (eds). 1995. *USDA-water erosion prediction project hillslope profile and watershed model documentation*. NSERL Report 10, National Soil Erosion Laboratory, West Lafayette, IN.

Freeze RA. 1980. A stochastic-conceptual analysis of rainfall-runoff processes on a hillslope. *Water Resources Research* **16**: 391–408.

Gao X, Sorooshian S, Goodrich DC. 1993. Linkage of a GIS to a distributed rainfall-runoff model. In *Environmental Modeling with GIS*, Goodchild MF, Parks BO, Steyaert LT (eds). Oxford University Press: New York; 182–187.

Goodrich DG, Woolhiser DA, Keefer TO. 1991. Kinematic routing using finite elements on a triangular irregular network. *Water Resources Research* **27**: 995–1003.

Grayson RB, Moore ID, McMahon TA. 1992a. Physically based hydrologic modeling 1. A terrain-based model for investigative purposes. *Water Resources Research* **28**: 2639–2658.

Grayson RB, Moore ID, McMahon TA. 1992b. Physically based hydrologic modeling 2. Is the concept realistic? *Water Resources Research* **28**: 2659–2666.

Howes DA, Abrahams AD. 2003. Modeling runoff and runon in a desert shrubland ecosystem, Jornada basin, New Mexico. *Geomorphology* **53**: 45–73.

Martinez-Meza E, Whitford WG. 1996. Stemflow, throughfall and channelization of stemflow by roots in three Chihuahuan desert shrubs. *Journal of Arid Environments* **32**: 271–287.

Moore ID, Grayson RB. 1991. Terrain-based catchment partitioning and runoff prediction using vector elevation data. *Water Resources Research* **27**: 1177–1191.

Navar J, Bryan R. 1990. Interception loss and rainfall redistribution by three semi-arid growing shrubs in northeastern Mexico. *Journal of Hydrology* **115**: 51–63.

Nielsen DR, Biggar JW, Erh KT. 1973. Spatial variability of field measured soil-water properties. *Hilgardia* **42**: 215–260.
Noy-Meir I. 1985. Desert ecosystem structure and function. In *Hot Deserts and Arid Shrublands*, Evanari M, Noy-Meir I, Goodall DW (eds). Elsevier: Amsterdam; 93–103.
Onstad CA, Brakensiek DL. 1968. Watershed simulation by the stream path analogy. *Water Resources Research* **4**: 965–971.
Parsons AJ, Wainwright J, Abrahams AD, Simanton JR. 1997. Distributed dynamic modelling of interrill overland flow. *Hydrological Processes* **11**: 1838–1859.
Ponce VM. 1991. The kinematic wave controversy. *Journal of Hydraulic Engineering* **117**: 511–525.
Refsgaard JC. 1997. Parameterisation, calibration and validation of distributed hydrological models. *Journal of Hydrology* **198**: 69–97.
Refsgaard JC, Storm B. 1996. Construction, calibration and validation of hydrological models. In *Distributed Hydrological Modelling*, Abbott MB, Refsgaard JC (eds). Kluwer: Dordrecht, The Netherlands; 41–54.
Reynolds JF, Virginia RA, Schlesinger WH. 1997. Defining functional types for models of desertification. In *Plant Functional Types: Their Relevance to Ecosystem Properties and Global Change*, Smith TM, Shugart HH, Woodward FI (eds). Cambridge University Press: Cambridge, UK; 194–214.
Saint Venant B de. 1871. Theory of unsteady water flow, with application to river floods and to propagation of tides in river channels. *French Academy of Science* **73**.
Schlesinger WH, Jones CS. 1984. The comparative importance of overland runoff and mean annual rainfall to shrub communities of the Mojave Desert. *Botanical Gazette* **145**: 116–124.
Schlesinger WH, Abrahams AD, Parsons AJ, Wainwright J. 1999. Nutrient losses in runoff from grassland and shrubland habitats in southern New Mexico: 1. Rainfall simulation experiments. *Biogeochemistry* **45**: 21–34.
Scoging HM, Parsons AJ, Abrahams AD. 1992. Application of a dynamic overland-flow hydraulic model to a semi-arid hillslope, Walnut Gulch, Arizona. In *Overland Flow Hydraulics and Erosion Mechanics*, Parsons AJ, Abrahams AD (eds). UCL Press: London, UK; 105–145.
Sherman B, Singh VP. 1976. A distributed converging overland flow model: 1. Mathematical solutions. *Water Resources Research* **12**: 889–896.
Singh VP. 1996. *Kinematic Wave Modeling in Water Resources: Surface-Water Hydrology*. John Wiley: New York.
Smith RE, Parlange J-Y. 1978. A parameter-efficient hydrologic infiltration model. *Water Resources Research* **14**: 533–538.
Smith RE, Goodrich DG, Woolhiser DA, Unkrich CL. 1995. KINEROS—KINematic runoff and EROSion model. In *Computer Models of Watershed Hydrology*, Singh VP (ed.). Water Resources Publications: Fort Collins, CO; 697–732.
Springer EP, Cundy TW. 1987. Field scale evaluation of infiltration parameters from soil texture for hydrologic analysis. *Water Resources Research* **23**: 325–341.
Tarboton DG. 1997. A new method for the determination of flow directions and upslope areas in grid digital elevation models. *Water Resources Research* **33**: 309–319.
Vertessy RA, Hatton TJ, O'Shaughnessy PJ, Jayasuriya MDA. 1993. Predicting water yield from a mountain ash forest catchment using a terrain analysis based catchment model. *Journal of Hydrology* **150**: 665–700.
Woolhiser DA, Smith RE, Goodrich DC. 1990. *KINEROS: A Kinematic Runoff and Erosion Model: Documentation and User Manual*. US Department of Agriculture, Agricultural Research Service Report No. 77, Fort Collins, CO.
Zhang W, Cundy TW. 1989. Modeling of two-dimensional overland flow. *Water Resources Research* **25**: 2019–2035.

